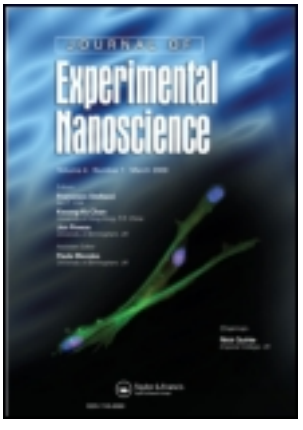

Journal of Experimental Nanoscience
Publication details, including instructions for authors and subscription information:
http://www.tandfonline.com/loi/tjen20

Magnetisation behaviour of mixtures of ferrofluids and paramagnetic fluids with same particle volume fractions

Rongli Gao [a], Jian Li [a], Shaona Han [a], Bangcai Wen [a], Tingzhen Zhang [a], Hua Miao [a] & Qingmei Zhang [a]

[a] MOE Key Laboratory on Luminescence and Real-Time Analysis, School of Physical Science and Technology, Southwest University, Chongqing 400715, P.R. China

Version of record first published: 30 Mar 2011.

To cite this article: Rongli Gao , Jian Li , Shaona Han , Bangcai Wen , Tingzhen Zhang , Hua Miao & Qingmei Zhang (2012): Magnetisation behaviour of mixtures of ferrofluids and paramagnetic fluids with same particle volume fractions, Journal of Experimental Nanoscience, 7:3, 282-297

To link to this article: http://dx.doi.org/10.1080/17458080.2010.524668

Journal of Experimental Nanoscience
Vol. 7, No. 3, May–June 2012, 282–297

Taylor & Francis
Taylor & Francis Group

Magnetisation behaviour of mixtures of ferrofluids and paramagnetic fluids with same particle volume fractions

Rongli Gao, Jian Li*, Shaona Han, Bangcai Wen, Tingzhen Zhang, Hua Miao and Qingmei Zhang

MOE Key Laboratory on Luminescence and Real-Time Analysis, School of Physical Science and Technology, Southwest University, Chongqing 400715, P.R. China

(*Received 25 March 2010; final version received 1 September 2010*)

In this study, γ-Fe_2O_3 ferrimagnetic nanoparticles and paramagnetic nanoparticles of p-$MgFe_2O_4$ (a hydroxide precursor for the preparation of magnesium ferrite materials) are produced by chemical precipitation technology. The γ-Fe_2O_3 ferrofluids and p-$MgFe_2O_4$ paramagnetic fluids are synthesised by Massart's method. The binary ferrofluids are obtained by mixing the ferrofluids and the paramagnetic fluids. There is insufficient magnetic interaction to aggregate the γ-Fe_2O_3 ferrimagnetic system and the p-$MgFe_2O_4$ paramagnetic system, so the magnetisation behaviour of the binary ferrofluids can be explored with reference to those of the single fluids. The magnetisation behaviour of single γ-Fe_2O_3 ferrofluids may be described by a model of gas-like compression. In the absence of a magnetic field, some particles can self-assemble into aggregates with a closed ring-like structure which make no contribution to the magnetisation of the γ-Fe_2O_3 ferrofluids. These ring-like aggregates result in the measured saturation magnetisation of the γ-Fe_2O_3 ferrofluids being smaller than the theoretical value calculated from the particles. During the magnetisation process, the polarised p-$MgFe_2O_4$ particles gas can orient the rings towards the direction of the field, so that the rings may fragment. Therefore, the measured saturation magnetisation of the γ-Fe_2O_3 ferrofluid component of the binary ferrofluids strengthens and the magnetisation process becomes easier than for pure γ-Fe_2O_3 ferrofluids.

Keywords: ferrofluids; paramagnetic fluids; binary; magnetisation

1. Introduction

Ferrofluids are colloidal suspensions of single-domain strong magnetic (ferromagnetic or ferrimagnetic) particles with diameters around 10 nm. These particles are dispersed in a carrier liquid and stabilised against agglomeration by long-chain surfactants (steric repulsion) or by attached ions (electrostatic repulsion) [1]. Ferrofluids have been the subject of many research works due to their variety of possible practical applications. In recent years, a bidisperse theoretical model, which contains two sizes of particles, large and small, with the same chemical composition has been proposed [2–6]. It has been

*Corresponding author. Email: aizhong@swu.edu.cn

ISSN 1745–8080 print/ISSN 1745–8099 online

http://dx.doi.org/10.1080/17458080.2010.524668
http://www.tandfonline.com

determined that the large particles provide the main field-induced structure of the ferrofluids under an external field and the small particles either suppress or enhance the formation and variation of the field-induced structure, depending on the proportion present. It is expected that ferrofluids with bidispersed sizes may have some properties that are different from ferrofluids with a distribution of sizes. However, such a bidispersed system is difficult to achieve experimentally. Generally, the saturation magnetisation of the ferrimagnetic component M_s is far greater than the induced magnetisation of the paramagnetic component M ($=\chi H$). Accordingly, fluids composed of ferrimagnetic and paramagnetic nanoparticles can be considered as magnetically bidispersed ferrofluids. In this ferrofluid, the magnetic phase is composed of two kinds of magnetic particles, strong magnetic particles and weak magnetic particles, so it can be called a 'binary ferrofluid'. In this article, binary γ-Fe_2O_3–p-$MgFe_2O_4$ ferrofluids are prepared by directly mixing strong magnetic γ-Fe_2O_3 ferrofluids and weak magnetic p-$MgFe_2O_4$ paramagnetic fluids. Their magnetisation behaviour is studied.

2. Experimental

2.1. *Preparation of the particles*

The γ-Fe_2O_3 particles and the precursor of the $MgFe_2O_4$ particles (a mixture of both $Mg(OH)_2$ and $Fe(OH)_3$, denoted p-$MgFe_2O_4$ in this article) are prepared by co-precipitation [7,8]. The p-$MgFe_2O_4$ particles are prepared as follows: $FeCl_3$ (0.04 mol) and $Mg(NO_3)_2$ (0.02 mol) are dissolved in 50 mL of pure water. The mixed metal solution is then added to a Na(OH) (0.7 mol/L, 500 mL) solution, heated to boiling point with stirring, the boiling is continued for 5 min, and then the mixture cooled to room temperature. The precipitate is washed with very dilute aqueous solution of HNO_3 (0.01 mol/L) until the pH of the washed solution is 7. Finally, the precipitate is added to $Fe(NO_3)_3$ solution (0.5 mol/L, 300 mL), heated to boiling and held at this temperature for up to 30 min before being allowed to cool naturally to room temperature. The precipitate is then dehydrated with acetone, dried at room temperature and ground. The method of preparing γ-Fe_2O_3 nanoparticles is quite similar to that of p-$MgFe_2O_4$ particles, except that Mg $(NO_3)_2$ is replaced by $FeSO_4{\cdot}(NH_4)_2SO_4$ and the amount of Na(OH) solution is less (0.42 mol/L, 500 mL).

2.2. *Synthesis and characteristics of the fluids*

Using Massart's method [9], the γ-Fe_2O_3 and p-$MgFe_2O_4$ particles are used to produce fluids in which the particle volume fraction $\phi = 0.4\%$, 0.8%, 1.2% and 1.6%, respectively, by diluting with the mother fluid ($\phi = 2\%$). Then, equal volumes of the two fluids having the same particle volume fractions are mixed, to give the binary ferrofluids.

According to the definition of the particle volume fraction, it is expressed for the γ-Fe_2O_3–p-$MgFe_2O_4$ binary ionic fluids, ϕ_b, as

$$\phi_b = \frac{V_1}{V_1 + V_2} = \frac{\phi_\gamma V_\gamma + \phi_p V_p}{V_\gamma + V_p}, \tag{1}$$

where V_1 is the total volume of all particles, V_2 is the volume of carrier liquid, ϕ_γ and ϕ_p the particle volume fractions in the γ-Fe_2O_3 and p-$MgFe_2O_4$ mother fluids, and V_γ and V_p

the γ-Fe_2O_3 and p-$MgFe_2O_4$ mother fluid volumes used to synthesise the binary fluids, respectively.

As the volumes of both mother fluids are the same ($V_p = V_\gamma$), the particle volume fraction in the binary ferrofluids is

$$\phi_b = (\phi_\gamma + \phi_p)/2. \tag{2}$$

Thus, when $\phi_\gamma = \phi_p = \phi$, $\phi_b = \phi$.

The crystal structure and chemical elements of the particles are analysed by X-ray diffraction (XRD, XD-3), and energy dispersive X-ray spectroscopy (EDX, TN-II). Their morphology and sizes are examined by transmission electron microscopy (TEM, JEM-100CX2). The density of the fluids is determined with a density bottle. The magnetisation curves of γ-Fe_2O_3 and p-$MgFe_2O_4$ particles, and the γ-Fe_2O_3, p-$MgFe_2O_4$ and γ-Fe_2O_3–p-$MgFe_2O_4$ fluids are measured by a HH-15 vibrating sample magnetometer (VSM) under an applied field of up to 1 T at room temperature.

3. Experimental results and analysis

3.1. *XRD and EDX measurements*

The XRD spectra of the γ-Fe_2O_3 and p-$MgFe_2O_4$ particles are shown in Figure 1(a). The EDX spectrum of p-$MgFe_2O_4$ particles is shown in Figure 1(b), and the results of the quantitative analysis are listed in Table 1. It can be concluded from the XRD diffraction that the peaks of γ-Fe_2O_3 are very evident while the p-$MgFe_2O_4$ exhibits some blurry peaks because of poor crystallisation. The EDX analysis shows that molar ratio between Fe and Mg is about 9 : 1, rather than the value 2 : 1 as for the $MgFe_2O_4$ particles.

3.2. *Particle morphology and size*

Figure 2 is a typical TEM photograph of the p-$MgFe_2O_4$ and γ-Fe_2O_3 particles, and shows that the particles are basically spherical. The statistical analysis shows that the particle size distribution satisfies a log normal distribution. This distribution is considered to be the most appropriate for the treatment of particle sizes [10]. The size distribution function $f(\ln x)$ can be represented as:

$$f(\ln x) = \frac{1}{\sqrt{2\pi}\ln\sigma_g}\exp\left[-\frac{\ln^2(x/x_g)}{2\ln^2\sigma_g}\right], \tag{3}$$

where x, x_g and $\ln\sigma_g$ are the particle diameter, geometric mean diameter and standard deviation, respectively. The x has same dimensional magnitude (nm) as x_g. For a spherical particle system, x_g and $\ln\sigma_g$ show the most probable diameter and the dispersivity of the diameter, respectively. It can be concluded from the statistical analysis that the values of x_g for the p-$MgFe_2O_4$ and γ-Fe_2O_3 particles are 5.58 and 8.39 nm, and the standard deviations $\ln\sigma_g$ for the p-$MgFe_2O_4$ and γ-Fe_2O_3 particles are 0.39 and 0.29, respectively. Thus, the size distribution functions of p-$MgFe_2O_4$ and γ-Fe_2O_3 particles can be written as formulae (4) and (5), respectively,

$$f(\ln x) = 1.03\exp\left[-3.35\ln^2(x/5.58)\right], \tag{4}$$

$$f(\ln x) = 1.38\exp\left[-5.99\ln^2(x/8.39)\right]. \tag{5}$$

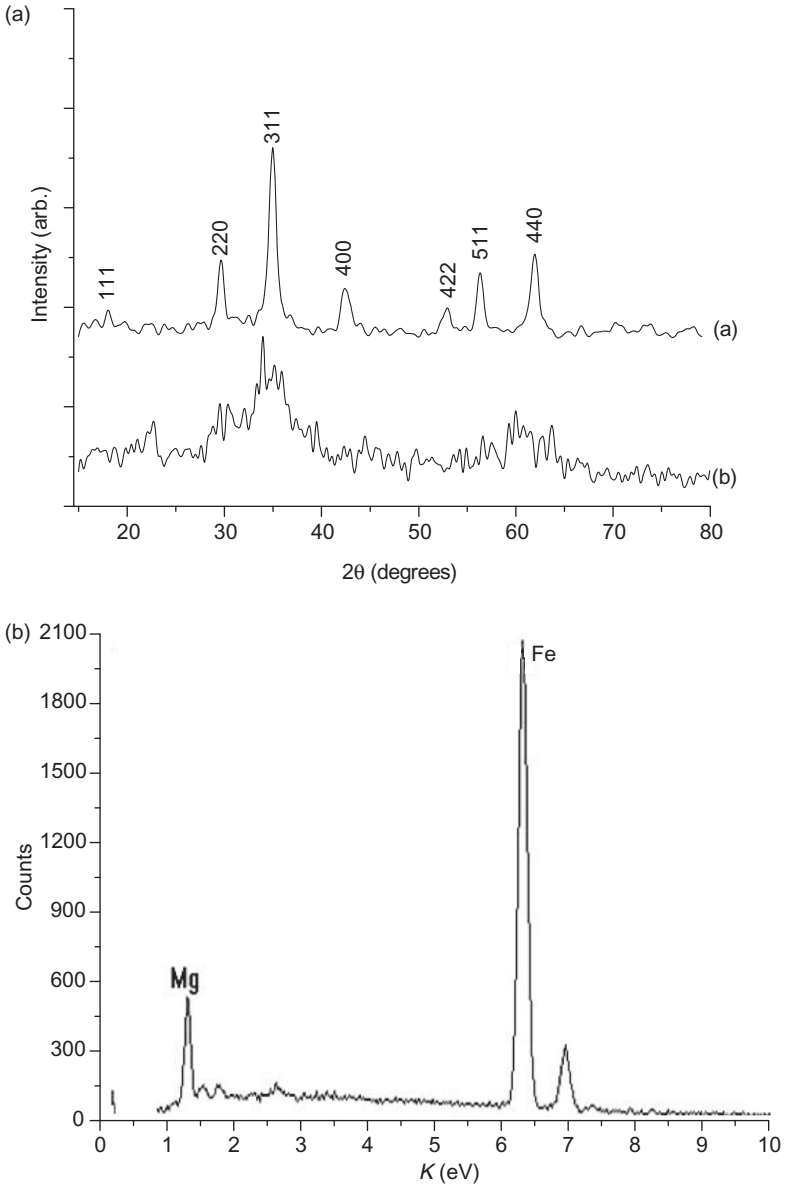

Figure 1. (a) XRD spectra of (a) γ-Fe_2O_3 particles, (b) p-$MgFe_2O_4$ particles and (b) EDX spectrum of p-$MgFe_2O_4$ particles.

Table 1. Quantitative analysis of the p-$MgFe_2O_4$ particles using EDX.

Element	*K* ratio	ZAF correlation	Weight ratio (%)	Atom ratio (%)
Mg	0.02689	0.5360	4.4566	8.9518
Fe	0.97311	0.9782	95.5434	91.0482

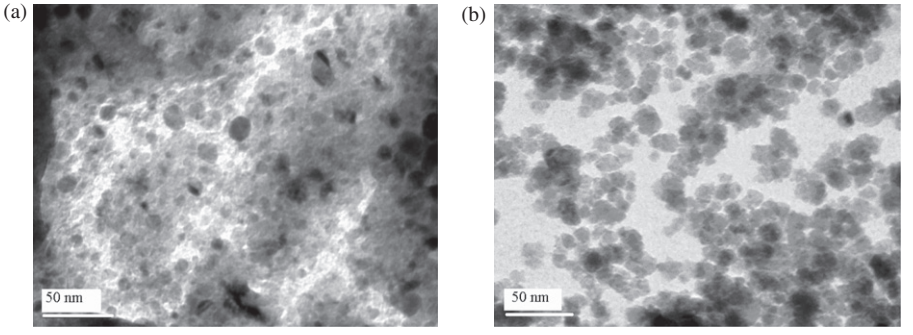

Figure 2. TEM photographs of (a) p-$MgFe_2O_4$ nanoparticles and (b) γ-Fe_2O_3 nanoparticles.

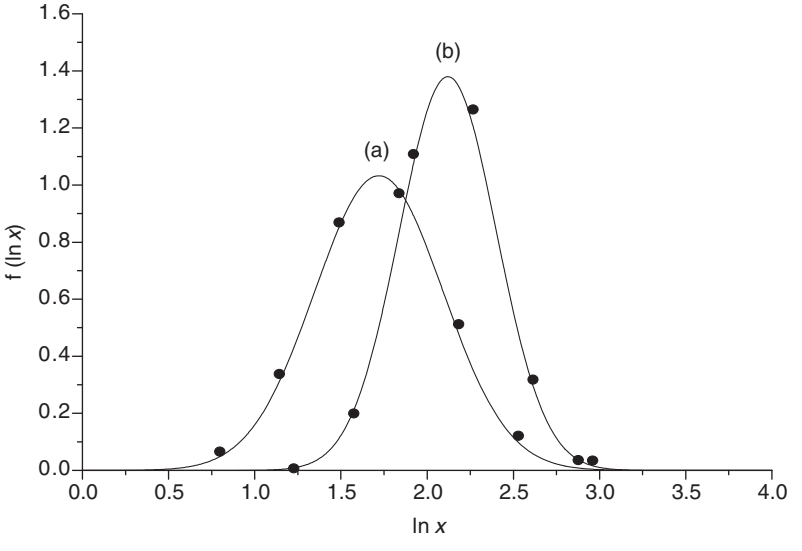

Figure 3. The size distribution for (a) p-$MgFe_2O_4$ particles and (b) γ-Fe_2O_3 particles: • experimental data; —— fitted theoretical curve.

The experimental data and distribution curves from the theoretical fitting are illustrated in Figure 3.

3.3. *Particle density*

The particles and the carrier liquid are assumed to be mixed simply without wetting. Thus, the densities of the fluids can be described by

$$\rho_f = (\rho - \rho_c) \cdot \phi + \rho_c, \tag{6}$$

where ρ_f, ρ and ρ_c are the densities of the fluid, particle and carrier liquid, respectively, and ϕ is the particle volume fraction. The density of carrier liquids is measured to be

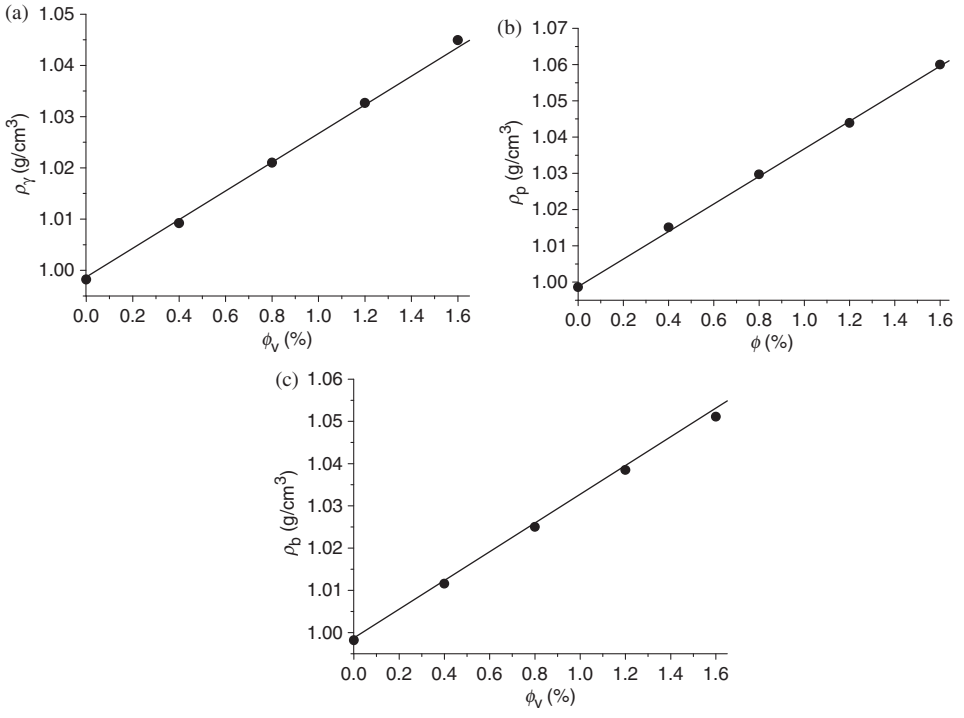

Figure 4. Density variation of fluids as a function of the particle volume fraction at room temperature (a) p-$MgFe_2O_4$, (b) γ-Fe_2O_3 and (c) γ-Fe_2O_3–p-$MgFe_2O_4$: • experimental data; —— fitted theoretical curve.

0.9982 g/cm^3 at room temperature. The p-$MgFe_2O_4$ particles can be looked upon as a material formed from a mixture of $Fe(OH)_3$ and $Mg(OH)_2$ with molar ratio about 9 : 1. Therefore, the density of the p-$MgFe_2O_4$ particles ρ_p can be expressed as

$$\rho_p = (9\rho_{Fe} + 1\rho_{Mg})/10, \tag{7}$$

where ρ_{Fe} and ρ_{Mg} are the densities of $Fe(OH)_3$ and $Mg(OH)_2$, 4.0 and 2.5 g/cm^3, respectively. Thus, the density of the p-$MgFe_2O_4$ particle is calculated to be 3.85 g/cm^3 according to formula (7). The γ-Fe_2O_3–p-$MgFe_2O_4$ binary fluids are mixed with γ-Fe_2O_3 and p-$MgFe_2O_4$ fluids with volume ratio 1 : 1, so the average density of the particles in the γ-Fe_2O_3–p-$MgFe_2O_4$ binary fluids ρ_b can be expressed as

$$\rho_b = (\rho_p + \rho_r)/2, \tag{8}$$

where ρ_γ is the density of the γ-Fe_2O_3 particles, 4.86 g/cm^3. Thus, the density ρ_b is calculated to be 4.36 g/cm^3. The experimental and theoretical densities of p-$MgFe_2O_4$, γ-Fe_2O_3 and the binary fluids as a function of particle volume fraction are shown in Figure 4. It can be seen that the theoretical curves are in agreement with the experimental data. These indicate that the values of ρ_p and ρ_b are correct.

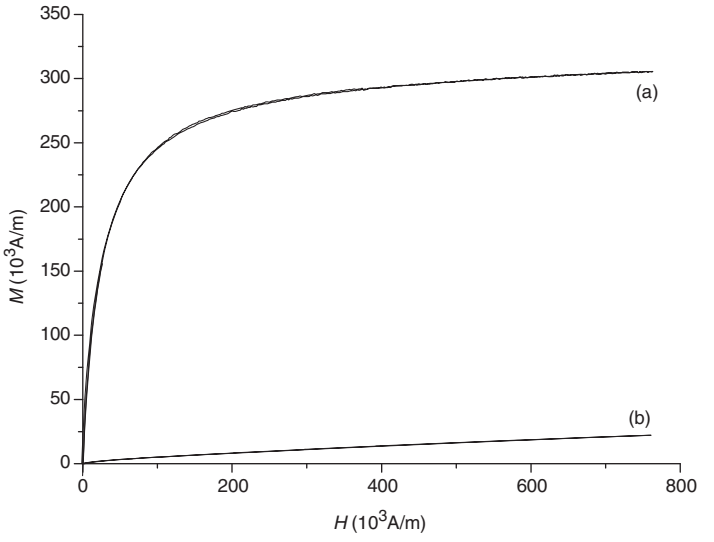

Figure 5. Magnetisation curves as a function of the applied field of (a) γ-Fe_2O_3 particles and (b) p-$MgFe_2O_4$ particles.

3.4. *Magnetisation measurements*

In these measurements, the magnetisation per unit mass σ is measured since it is easier to accurately measure mass [11]. The magnetisation per unit volume is given by

$$M = \sigma \cdot \rho, \tag{9}$$

where ρ is the density of the material measured. The magnetisation curves of the two particles are shown in Figure 5. Clearly, the γ-Fe_2O_3 particle is strongly magnetic, exhibiting ferrimagnetic behaviour, and the p-$MgFe_2O_4$ nanoparticle is a weakly magnetic particle which is paramagnetic. According to the relationship $M \sim 1/H$ at high field, the saturation magnetisation of γ-Fe_2O_3 M_s can be estimated to be 321.72 kA/m, by extrapolating the line $M \sim 1/H$ to $1/H = 0$. The magnetisation is far larger than the magnetisation of p-$MgFe_2O_4$ (17.15 kA/m) when the field is 1 T. The susceptibility of the p-$MgFe_2O_4$ particle, χ_p, is 0.031.

The magnetisation curves of the two single component and binary ferrofluids with different particle volume fractions are shown in Figure 6. From Figure 6, it can be seen that the magnetisation behaviour of p-$MgFe_2O_4$ and γ-Fe_2O_3 fluids is similar to that of p-$MgFe_2O_4$ and γ-Fe_2O_3 particles, respectively, whilst the binary γ-Fe_2O_3–p-$MgFe_2O_4$ fluids have magnetisation behaviour similar to γ-Fe_2O_3 ferrofluids.

4. Discussion

4.1. *The magnetisation behaviour of the single fluids*

The p-$MgFe_2O_4$ nanoparticles are paramagnetic particles without permanent moments. Application of an external magnetic field induces a dipole moment in each particle and the

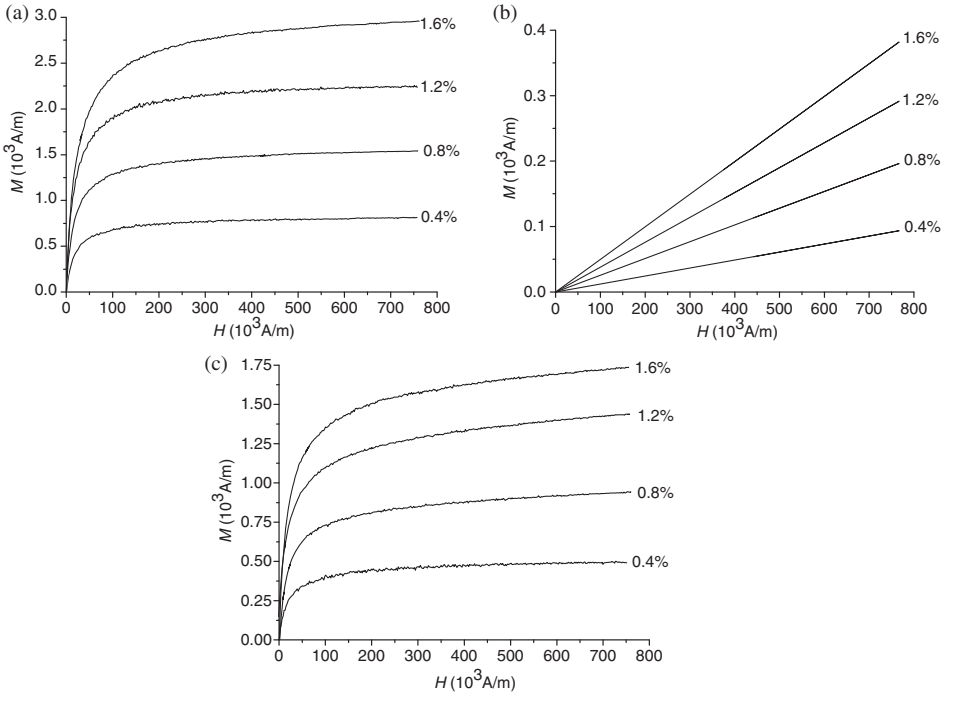

Figure 6. Magnetisation curves as a function of applied field for different particle volume fractions in (a) γ-Fe_2O_3 ferrofluids, (b) p-$MgFe_2O_4$ paramagnetic fluids and (c) the γ-Fe_2O_3–p-$MgFe_2O_4$ binary ferrofluids.

magnetisation is proportional to the external field in the experiments. The greatest average magnetic moment in the magnetic field is

$$\langle m\rangle = \frac{\pi}{6} M_{1\mathrm{T}} \int_0^\infty x^3 f(x)\mathrm{d}x, \tag{10}$$

where $M_{1\mathrm{T}}$ is the magnetisation at 1T. From the value of $M_{1\mathrm{T}}$ and the size distribution function of the p-$MgFe_2O_4$ particles from formula (4), the average moment of the p-$MgFe_2O_4$ particles is calculated to be $2.21 \times 10^{-21}(\mathrm{Am}^2)$, γ-Fe_2O_3 particles are ferromagnetic. Using the size distribution function from formula (5), the average magnetic moment is

$$\langle m\rangle = \frac{\pi}{6} M_s \int_0^\infty x^3 f(x)\mathrm{d}x = 1.92 \times 10^{-19}(\mathrm{Am}^2).$$

The magnetic interaction between the magnetic nanoparticles can be regarded as the interaction between magnetic moments. Therefore, the interaction energy between particle i and particle j is given by

$$E = \mu_0\left[\mathbf{m}_i \cdot \mathbf{m}_j - 3(\mathbf{r}_{ij}/\mathbf{r}_{ij} \cdot \mathbf{m}_i)(\mathbf{r}_{ij}/\mathbf{r}_{ij} \cdot \mathbf{m}_j)\right]/4\pi r_{ij}^3, \tag{11}$$

Table 2. Measured and calculated susceptibility (χ_f and $\phi_p \cdot \chi_p$) for p-$MgFe_2O_4$ paramagnetic fluids with different particle volume fractions ($\chi_p = 0.031$).

ϕ_p (%)	0.4	0.8	1.2	1.6
χ_f (10^{-4})	1.22	2.56	3.80	4.98
$\phi_p \cdot \chi_p$ (10^{-4})	1.24	2.48	3.72	4.96

where μ_0 is the vacuum permeability, m_i and m_j are the moments corresponding to the particles i and j, respectively, and r_{ij} is the distance between particle i and particle j. When the angles between the direction of the magnetic moments and the central line are zero, i.e. $\mathbf{r}_{ij}/r_{ij} \cdot \mathbf{m}_i = m_i$ and $\mathbf{r}_{ij}/r_{ij} \cdot \mathbf{m}_j = m_j$, two p-$MgFe_2O_4$ particles ($r_{ij} = d = 5.58$ nm) linked by contact give the greatest interaction energy, about 5.67×10^{-24} J. The interaction energy between two γ-Fe_2O_3 particles ($r_{ij} = d = 8.39$ nm) is about 1.248×10^{-20} J. When one p-$MgFe_2O_4$ particle and one γ-Fe_2O_3 particle are linked by contact ($r_{ij} = (d_\gamma + d_p)/2$, where d_γ and d_p are the average diameters of γ-Fe_2O_3 and p-$MgFe_2O_4$ particles), the interaction energy is about 2.51×10^{-22} J. The thermal energy ($=k_B T$) is about 4.14×10^{-21} J at room temperature ($T = 300$ K). As regards the p-$MgFe_2O_4$ fluids, the interaction energy between the particles is far smaller than the thermal energy for the field of the experiments, so the particles cannot form aggregates in the process of magnetisation, thus the magnetisation M_f can be described as

$$M_f = \chi_f H, \quad \chi_f = \phi_p \cdot \chi_p, \tag{12}$$

where, χ_f and χ_p are the susceptibility of the fluids and the particles, respectively, H is the applied field and ϕ_p is the particle volume fraction in the p-$MgFe_2O_4$ paramagnetic fluid. The relationship between the susceptibility and the particle volume fraction is given in Table 2. It can be seen that the calculated values of $\phi_p \chi_p$ are consistent with the measured values of χ_f and the susceptibility of the p-$MgFe_2O_4$ fluids shows a linear relationship to the particle volume fraction. These indicate that the magnetisation behaviour of p-$MgFe_2O_4$ fluids is the same as the particles.

For γ-Fe_2O_3 ferrofluids, the relationship of the saturation magnetisation between the ferrofluids and the particles should be

$$M_{f.s} = \phi_\gamma M_{p.s}, \tag{13}$$

where, $M_{f.s}$ is the saturation magnetisation of the γ-Fe_2O_3 ferrofluid, $M_{p.s}$ is the saturation magnetisation of the γ-Fe_2O_3 particles and ϕ_γ is the particle volume fraction in the ferrofluid. It can be determined from formula (13) that the magnetisation ($M_{f.s}$) and the particle volume fraction (ϕ_γ) should form a linear relationship. The measured and theoretical saturation magnetisations of γ-Fe_2O_3 ferrofluids with different volume fractions are given in Table 3 from which it can be concluded that the measured saturation magnetisations of γ-Fe_2O_3 ferrofluids are smaller than the theoretical values, i.e. $M_{f.s} < \phi_\gamma M_{p.s}$. This means that in the absence of a magnetic field, some γ-Fe_2O_3 particles in the ferrofluids can self-assemble into aggregates with ring-like structures to minimise the magnetic energy [12–15]. In the self-assembled aggregates, the magnetic flux is closed and makes no contribution to the magnetisation [15]. It can be seen from Table 3 that the proportion of ring-like structures increase with the particle volume fraction.

Table 3. Measured and theoretical saturation magnetisation of γ-Fe_2O_3 ferrofluids with different particle volume fractions.

ϕ (%)	0.4	0.8	1.2	1.6
$M_{f.s}$ (10^3 A/m)	0.85	1.60	2.31	3.05
ϕ. $M_{p.s}$ (10^3 A/m)	1.28	2.57	3.86	5.14
$\frac{M_{f.s}}{\phi M_{p.s}}$ (%)	66	62	60	59

Note: $M_{p.s} = 321.72\,\text{kA/m}$.

In the absence of an external magnetic field, for ferrofluids, the average distance between particles L can be estimated by $L = d \cdot \sqrt[3]{\phi^{-1}\pi/6}$, where d is the diameter of the particles [16]. For $CoFe_2O_4$ ferrofluids, taking $d = x_g = 8.39\,\text{nm}$, L can be calculated as 25 nm while $\phi = 2\%$ (mother fluid). The distance is more than the sum of the two particles' radius. Therefore, the physical contact of the particles, which would induce the irreversible coagulation, can be unconsidered. Under the influence of an external magnetic field, if the intrinsic magnetic dipole–dipole interaction can be neglected and the particle diameters are equal, the magnetisation of the ferrofluids M can be described by the Langevin function

$$M = M_{f.s}L(\alpha), \quad \alpha = \mu_0 \pi M_{p.s} d^3 H/6kT, \tag{14}$$

where $M_{f.s}$ the saturation magnetisation of the ferrofluid, M_s is the saturation magnetisation of the particles, $L(\alpha) = \coth(\alpha) - 1/\alpha$ is the Langevin function, μ_0 is the vacuum permeability, d is the average diameter of the particles, H is the magnetic intensity, k is the Boltzmann constant and T is the absolute temperature. In order to consider the effect of the field-induced aggregates on the magnetisation of the ferrofluids, a model of gas-like compression (MGC) has been proposed [17] and the relationship between the magnetisation and the applied magnetic field is described as

$$\begin{aligned} M &= M_{f.s}\left(\coth(\alpha) - \frac{1 + \ln(\varphi_H/\varphi)}{\alpha}\right) \\ &= M_{f.s}\left(L(\alpha) - \frac{\ln(\varphi_H/\varphi)}{\alpha}\right). \end{aligned} \tag{15}$$

In formula (15), ϕ_H is the particle volume fraction in the field-induced aggregates as a function of magnetic field and is written as

$$\phi_H = (0.638 - \phi)\tanh\left(\gamma(\phi\alpha)^2\right) + \phi, \tag{16}$$

where the parameter γ is defined as a compression parameter and demonstrates the effect of aggregates on the magnetisation. If γ is taken as zero, formula (15) would become formula (14), which means that the field-induced interaction between the particles can be neglected during the magnetisation process. When the ferrofluids approach saturation magnetisation, formula (15) can be written as $M = M_{f.s}\,(1 - 1/\alpha)$ and is consistent with Langevin theory for the magnetisation process. The reduced magnetisation curves of γ-Fe_2O_3 ferrofluids with the following volume fractions, $\phi_\gamma = 0.4\%$, 0.8%, 1.2% and 1.6%, are shown in Figure 7. Clearly, the magnetisation process for the γ-Fe_2O_3 ferrofluids is more difficult to describe than by simple Langevin theory. This shows that

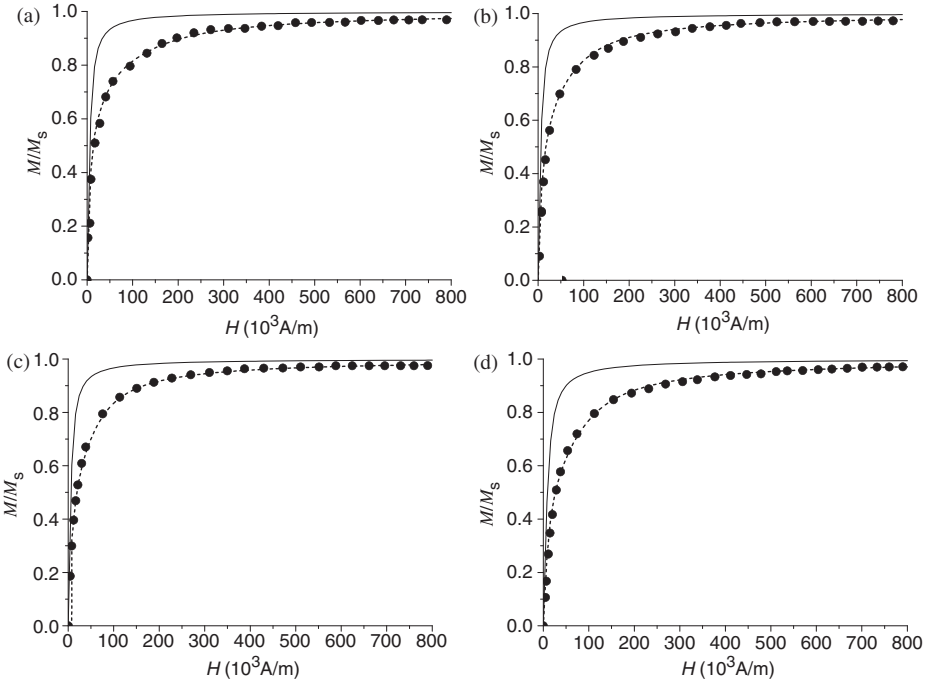

Figure 7. Reduced magnetisation curves of γ-Fe_2O_3 ferrofluids with different particle volume fractions: the experimental data (points); Langevin function (solid lines) and the MGC (dashed lines).

there is interaction among the γ-Fe_2O_3 particles when the ferrofluids are magnetised. The MGC can be fitted to the experimental data, as shown in Figure 7. The fitted results indicate that the compression parameter γ, i.e. the effect of field-induced aggregation on the magnetisation behaviour, increases with the particle volume fractions for the single γ-Fe_2O_3 ferrofluids.

4.2. *Magnetisation behaviour of the binary ferrofluids*

The binary γ-Fe_2O_3–p-$MgFe_2O_4$ ferrofluids were synthesised by mixing γ-Fe_2O_3 and p-$MgFe_2O_4$ fluids; there is not enough magnetic interaction to cause aggregation between the γ-Fe_2O_3 and p-$MgFe_2O_4$ particles. Therefore, when considering the magnetism of the binary ferrofluids, the magnetic interaction between the γ-Fe_2O_3 and p-$MgFe_2O_4$ particles can be neglected. Accordingly, to describe their magnetic behaviour, the binary ferrofluid systems can be divided into two subsystems corresponding to γ-Fe_2O_3 and p-$MgFe_2O_4$ fluids. Thus, the magnetisation of the binary ferrofluid M can be written as

$$M = yM_1 + (1 - y)M_2, \tag{17}$$

where, M_1 and M_2 are the magnetisations of the single γ-Fe_2O_3 and p-$MgFe_2O_4$ fluids, respectively, and y and $(1 - y)$ are the fractional volumes of γ-Fe_2O_3 and p-$MgFe_2O_4$ fluids in the total volume of the binary ferrofluid. Formula (17) means that for such a

binary ferrofluid system, the magnetisation resulting from nonmagnetic interaction between the two subsystems can be demonstrated by varying M_1 or/and M_2.

The γ-Fe_2O_3–p-$MgFe_2O_4$binary ferrofluids are synthesised by mixing equal volumes of the two single fluids; so y is 0.5. Thus,

$$M = 0.5M_1 + 0.5M_2. \tag{18}$$

The summed magnetisation can be re-written in terms of the experimental data as

$$M = 0.5M_\gamma + 0.5M_{\text{p-Mg}}, \tag{19}$$

where M_γ and $M_{\text{p-Mg}}$ are the measured magnetisations of the γ-Fe_2O_3 ferrofluids and p-$MgFe_2O_4$ paramagnetic fluids, respectively, or from the theoretical description as

$$M = 0.5M_{\text{f.s}}\left(\coth(\alpha) - \frac{1 + \ln(\varphi_H/\varphi_\gamma)}{\alpha}\right) + 0.5\chi_{\text{f}}H, \tag{20}$$

where $M_{\text{f.s}}$ is the saturation magnetisation of the γ-Fe_2O_3 ferrofluid and χ_{f} is the susceptibility of the p-$MgFe_2O_4$ paramagnetic fluid. The summed magnetisation of both the γ-Fe_2O_3 ferrofluids and p-$MgFe_2O_4$ paramagnetic fluids, and the measured magnetisation of the binary ferrofluids with volume fractions $\phi_{\text{v}} = 0.4\%$ (a), 0.8% (b), 1.2% (c) and 1.6% (d) are shown in Figure 8. It can be seen that in lower magnetic fields

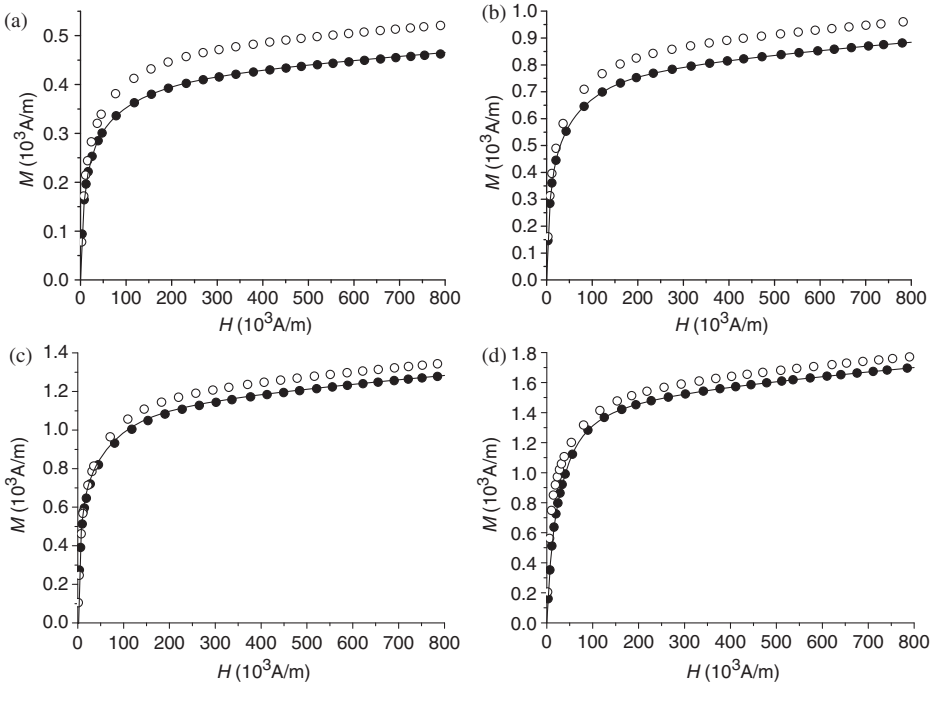

Figure 8. Measured magnetisation of ferrofluids (valid points), sum of magnetisation data from single γ-Fe_2O_3 and p-$MgFe_2O_4$ ferrofluids according to formula (19) (black points) and fitted magnetisation curves according to formula (20) (solid lines).

($H < 20\,\mathrm{kA/m}$) the experimental data for the binary ferrofluids agree with both formulae (19) and (20), but at a higher magnetic field ($H > 50\,\mathrm{kA/m}$) the measured magnetisations of the binary ferrofluids are stronger than the summed magnetisation of the γ-Fe_2O_3 ferrofluid and p-$MgFe_2O_4$ paramagnetic fluid (i.e. $M > 0.5(M_\gamma + M_\mathrm{p})$). This shows that the magnetisation behaviour of the binary ferrofluids is not a simple summation of those of the γ-Fe_2O_3 ferrofluids and p-$MgFe_2O_4$ paramagnetic fluids, and the magnetisation behaviour of the γ-Fe_2O_3 component of the binary ferrofluids is different from that in single γ-Fe_2O_3 ferrofluids. This indicates a microstructural transition of the γ-Fe_2O_3 system in the binary ferrofluids. Therefore, the characteristic parameters of the single γ-Fe_2O_3 ferrofluids $M_\mathrm{f.s}$ and γ have been varied to fit the measured magnetisation data of the binary ferrofluids. First, it was observed that the measured data and the summed results have different slopes for the binary ferrofluids in high field (see Figure 8). The magnetisation curve of the binary ferrofluids can be written as $M = M_\mathrm{f.s}(1 - 1/\alpha) + \chi_\mathrm{f} H$ in high field, so, it is judged that the apparent saturation magnetisation of the γ-Fe_2O_3 ferrofluids component $M_\mathrm{f.s}$ in the binary ferrofluids has increased. Thus, the value $M_\mathrm{f.s}$ of the γ-Fe_2O_3 ferrofluids is adjusted until the curves fit the experimental data at high field. The fitted values of the apparent saturation magnetisation of the γ-Fe_2O_3 ferrofluids $M'_\mathrm{f.s}$ are listed in Table 4. Second, the value of γ is replaced with γ' ($= \gamma + \Delta\gamma$) and the value of $\Delta\gamma$ varied until the fitted results agree with the experimental data for the binary ferrofluids. The values of γ' are also listed in Table 4 and the fitted curves are illustrated in Figure 9.

The magnetisation increment and the γ parameter decrement of the γ-Fe_2O_3 ferrofluid component of the binary ferrofluids could result from the breaking of the ring-like aggregates of self-assembled γ-Fe_2O_3 particles. This is interpreted as follows. In the γ-Fe_2O_3–p-$MgFe_2O_4$ binary ferrofluids, the ring-like aggregates of self-assembled γ-Fe_2O_3 particles remain stationary and some of the small and weakly magnetic p-$MgFe_2O_4$ particles act as a gas of particles [18] around the ring-like structures. In the magnetisation process, the moments are induced in the p-$MgFe_2O_4$ particles along the direction of the applied magnetic field and p-$MgFe_2O_4$ particles will act as a magnetically polarised gas. The polarised p-$MgFe_2O_4$ particles could produce a magnetic interaction with the ring-like aggregates of γ-Fe_2O_3 particles. The force on the ring may be non-uniform. Thus, the orientation of some of the rings could rotate so that they lie perpendicular to the direction of the field. In a high enough field, those rings oriented perpendicular to the applied magnetic field can fragment spontaneously into short chains along the direction of the field [19,20]. The short γ-Fe_2O_3 chains from the fragmented rings will then produce a contribution to the magnetisation. Therefore, the measured saturation magnetisation

Table 4. Apparent saturation magnetisation (10^3 A/m) and γ parameter of γ-Fe_2O_3 ferrofluids for both single ferrofluids and binary ferrofluids.

ϕ_γ (%)	0.4	0.8	1.2	1.6
Single ferrofluids ($0.5M_\mathrm{f.s}$)	0.43	0.80	1.16	1.53
Binary ferrofluids ($M'_\mathrm{f.s}$)	0.49	0.88	1.22	1.60
$\Delta M_\mathrm{f.s}$ ($M'_\mathrm{f.s}$–$0.5M_\mathrm{f.s}$)	0.06	0.08	0.06	0.07
γ	5	8	10	15
γ'	4	7	8	12
$-\Delta\gamma(=\gamma'-\gamma)$	1	1	2	3

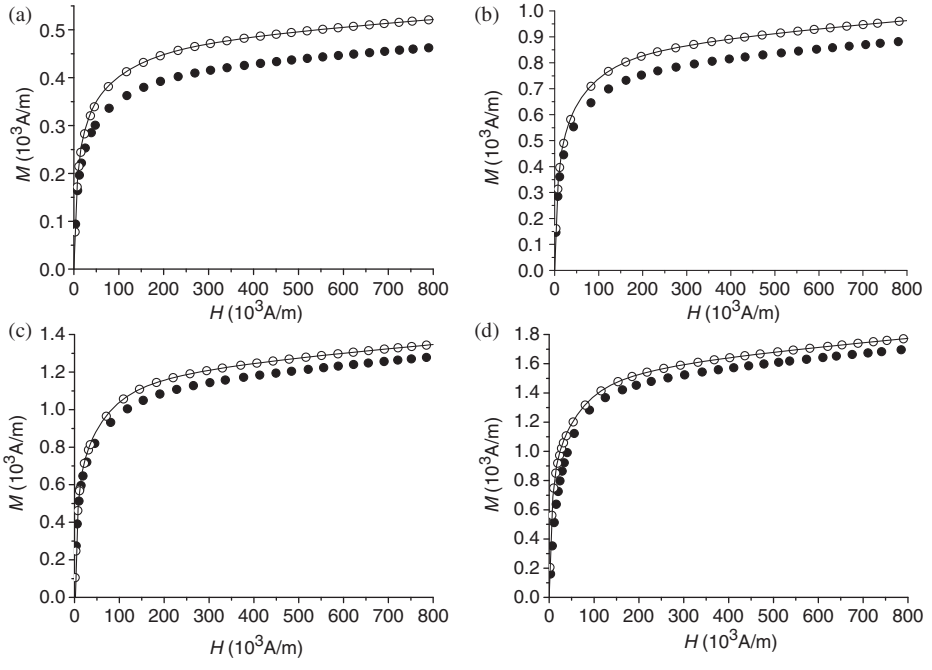

Figure 9. Summed magnetisation of the contributions from the γ-Fe_2O_3 and the p-$MgFe_2O_4$ ferrofluids (black points), measured magnetisation data of the binary ferrofluids (valid points), and fitted magnetisation curves from formula (20) after changing the apparent saturation magnetisation of the γ-Fe_2O_3 ferrofluid component $M_{f,s}$ (solid lines).

of the γ-Fe_2O_3 component will increase, consequently increasing the total magnetisation of the binary ferrofluids. Meanwhile, the fragmented ring-like aggregates, i.e. the effective moments that contribute to the magnetisation, increase gradually with the increase in the magnetic field. Thus, the magnetisation of the γ-Fe_2O_3 component of the binary ferrofluids is easier than the single γ-Fe_2O_3 ferrofluids, so that the γ apparently decreases. This means that the value of $\Delta\gamma$ reflects the increase of the effective moment, rather than a change of the field-induced aggregation behaviour.

5. Conclusions

The γ-Fe_2O_3 and p-$MgFe_2O_4$ nanoparticles are ferrimagnetic and paramagnetic, respectively. In this study, γ-Fe_2O_3–p-$MgFe_2O_4$ binary ferrofluids are synthesised by mixing together the γ-Fe_2O_3 ferrofluid and p-$MgFe_2O_4$ paramagnetic fluid, as prepared by Massart's method. The inherent moments of the γ-Fe_2O_3 particles are far larger than the induced moment of the paramagnetic p-$MgFe_2O_4$ particles in this experiment and there is insufficient magnetic interaction to form aggregates between the γ-Fe_2O_3 and p-$MgFe_2O_4$ subsystems. Therefore, the magnetisation behaviour of binary ferrofluids can be analysed based on those of the individual γ-Fe_2O_3 ferrofluid and p-$MgFe_2O_4$ paramagnetic fluid. In addition, the magnetisation behaviour of the binary ferrofluids mainly result from the

γ-Fe_2O_3 component. In the absence of a magnetic field, some γ-Fe_2O_3 particles can self-assemble into aggregates with a ring-like structure. These aggregates make no contribution to the magnetisation, so that the measured saturation magnetisation of the γ-Fe_2O_3 ferrofluids $M_{f.s}$ is less than $\phi_p M_{p.s}$. This means that for ferrofluids, the apparent saturation magnetisation measured does not correspond to moments of all particles being parallel. In the magnetisation process, the γ-Fe_2O_3 particles will form field-induced aggregates so that the magnetisation curves of the γ-Fe_2O_3 ferrofluids deviate from Langevin theory, although they can be described by the MGC. In the binary ferrofluids, the p-$MgFe_2O_4$ component acts in the same way as a gas of particles. Under an external applied magnetic field, the gas of polarised p-$MgFe_2O_4$ particles can reorient some of the γ-Fe_2O_3 particle rings so that the rings lie perpendicular to the direction of the applied magnetic field. As a result, some ring fragments and the apparent magnetisation of the γ-Fe_2O_3 ferrofluid component in the binary ferrofluids increase. The increased value of the magnetisation from the γ-Fe_2O_3 component is not related to the particle volume fraction. Since the proportion of fragmented rings gradually increases with the magnetic field, so does the effective inherent moment. This results in the apparent magnetisation of the γ-Fe_2O_3 component of the binary ferrofluid being easier than that of the pure γ-Fe_2O_3 ferrofluid. The effects of field-induced aggregate on the magnetisation behaviour of the pure γ-Fe_2O_3 ferrofluid and the binary ferrofluids are the same. To summarise, for the binary ferrofluids, the magnetisation behaviour results mainly from the γ-Fe_2O_3 component but the p-$MgFe_2O_4$ paramagnetic component can partially eliminate the self-assembled ring-like aggregates of γ-Fe_2O_3. This could be of considerable interest with respect to research into the physical behaviour and engineering applications of ferrofluids.

Acknowledgements

This study is supported by the National Natural Science Foundation Project of P.R. China (11074205).

References

[1] J. Li, D.L. Dai, X.D. Liu, Y.Q. Lin, Y. Huang, and L. Bai, *Preparation and characterization of self-formed $CoFe_2O_4$ ferrofluid*, J. Mater. Res. 22 (2007), pp. 886–892.

[2] J.P. Huang, Z.W. Wang, and C. Holm, *Structure and magnetic properties of mono- and bi-dispersed ferrofluids as revealed by simulations*, J. Magn. Magn. Mater. 289 (2005), pp. 234–237.

[3] A.Y. Zubarev and L.Yu. Iskakova, *Structural transformations in polydisperse ferrofluids*, Colloid. J. 65 (2003), pp. 778–787.

[4] G.M. Range and S.H.L. Klapp, *Density-functional study of the phase behavior of asymmetric binary dipolar mixtures*, Phys. Rev. E 69 (2004), pp. 041201-1–11.

[5] G.M. Range and S.H.L. Klapp, *Phase behavior of bidisperse ferrocolloids*, Phys. Rev. E. 70 (2004), pp. 061407-1–9.

[6] G.M. Range and S.H.L. Klapp, *Density-functional study of model bidisperse ferrocolloids in an external magnetic field*, J. Chem. Phys. 122 (2005), pp. 224902-1–6.

[7] R.L. Gao, J. Li, S.N. Han, Q. Li, and X.M. Chen, *The preparation of self-formed γ-Fe_2O_3 ferrofuids and its magnetism*, J. Southwest Uni. 30(5) (2008), pp. 1–7 (in Chinese).

[8] H. Aono, H. Hirazawa, T. Naohara, and T. Maehara, *Surface study of fine $MgFe_2O_4$ ferrite power prepared by chemical methods*, Appl. Surf. Sci. 254 (2008), pp. 2319–2324.
[9] R. Massart, *Preparation of aqueous magnetic liquids in alkaline and acidic media*, IEEE Trans. Mag. MAG-17 (1981), pp. 1247–1248.
[10] J. Popplewell and L. Sakhnini, *The dependence of the physical and magnetic properties of magnetic fluids on particle size*, J. Magn. Magn. Mater. 149 (1995), pp. 72–78.
[11] J. Crangle, *The Magnetic Properties of Solid*, Edward Arnold, London, 1977.
[12] P.J. Camp and G.N. Patey, *Structure and scattering in colloidal ferrofluids*, Phys. Rev. E 62 (2000), pp. 5403–5408.
[13] V.F. Puntes, K.M. Krishnan, and A.P. Alivisatos, *Colloidal nanocrystal shape and size control: The case of cobalt*, Science 291 (2001), pp. 2115–2117.
[14] C. Xu, Y.Q. Ma, P.M. Hui, and F.Q. Tong, *Microstructures in strongly interacting dipolar fluids*, Chin. Phys. Lett. 22 (2005), pp. 485–488.
[15] S. Taketomi, R.V. Drew, and R.D. Shull, *Peculiar magnetic aftereffect of highly diluted frozen magnetic fluids*, J. Magn. Magn. Mater. 307 (2006), pp. 77–84.
[16] G. Mériguet, M. Jardat, and P. Turq, *Structural properties of charge-stabilized ferrofluids under a magnetic field: A Brownian dynamics study*, J. Chem. Phys. 121 (2004), pp. 6078–6085.
[17] J. Li, Y. Huang, X.D. Liu, Y.Q. Lin, and L. Bai, *Effect of aggregates on the magnetization property of ferrofluids: A model of gaslike compression*, Sci. Technol. Adv. Mater. 8 (2007), pp. 448–454.
[18] R. Massart, E. Dubois, V. Cabuil, and E. Hasmonay, *Preparation and properties of monodisperse magnetic fluids*, J. Magn. Magn. Mater. 149 (1995), pp. 1–5.
[19] P. Jund, S.G. Kim, D. Tomanek, and J. Hetherington, *Stability and fragmentation of complex structures in ferrofluids*, Phys. Rev. Lett. 74 (1995), pp. 3049–3052.
[20] F. Kun, W. Wen, K.F. Pál, and K.N. Tu, *Breakup of dipolar rings under a perpendicular magnetic field*, Phys. Rev. E. 64 (2001), pp. 061503-1–8.